Unsaturated fatty acid synthesis is associated with poor prognosis in pediatric neuroblastoma and is differentially regulated by MYCN and tumor suppressor microRNAs.

Dennis A. Sheeter[1], Secilia Garza[2], Hui Gyu Park[1], Niharika R. Badi[1], Erika C. Espinosa[1], Kumar Kothapalli[3], J. Thomas Brenna[1,2,3], and John T. Powers[1,4]

[1]Dell Pediatric Research Institute and Department of Pediatrics, The University of Texas at Austin, Texas, 78723
[2]Dell Pediatric Research Institute and Department of Chemistry, The University of Texas at Austin, Texas, 78723
[3]Department of Nutritional Sciences, College of Natural Sciences, The University of Texas at Austin, Texas, 78723
[4]Division of Pharmacology and Toxicology, College of Pharmacy, The University of Texas at Austin, Texas, 78723

Correspondence,

J. T. Powers, john.powers@austin.utexas.edu
ORCID 0000-0003-1598-2417
J. T. Brenna, tbrenna@utexas.edu
ORCID 0000-0001-9494-4245

Email/ORCID
Dennis Sheeter, dennis.sheeter@austin.utexas.edu, ORCID 0009-0006-0412-0546
Secilia Garza, seci@utexas.edu, ORCID 0000-0001-9080-3410
Hui Gyu Park, hi.park@austin.utexas.edu, ORCID 0000-0002-0510-2095
Niharika Badi, NiharikaReddy.Badi@austin.utexas.edu
Erika Espinosa, ece97@austin.utexas.edu
Kumar Kothapalli, kkothapalli@utexas.edu, ORCID 0000-0003-0854-1023

Preprint submitted to bioRxiv, April 2023
Version 3.

ABSTRACT

MYCN amplification and disruption of tumor suppressor microRNA (TSmiR) function are central drivers of poor outcomes in neuroblastoma (NB). MYC, MYCN, and TSmiRs regulate glucose metabolism, yet their role in unsaturated fatty acid synthesis (UFAS) remains poorly understood. We show here that *de novo* and UFAS pathway genes *FASN*, *ELOVL6*, *SCD*, *FADS2*, and *FADS1* are upregulated in human NB and associate with poor prognosis. Consistent with this, we find that NB-related TSmiRs are predicted to extensively target these genes. In experiments with human NB cell lines, both MYC and MYCN upregulate UFAS pathway genes while suppressing TSmiR host gene expression, creating a possible UFAS regulatory network between *MYCN* and TSmiRs in NB. Further, NB cells are high in omega 9 (ω9) unsaturated fatty acids that can be synthesized *de novo*, and low in both ω6 and ω3, providing a plausible means for NB to limit cell-autonomous immune stimulation and reactive oxygen species (ROS)-driven apoptosis from ω6 and ω3 unsaturated fatty acid derivatives, respectively. We propose a model where the UFAS pathway, through novel regulation by *MYCN* and TSmiRs, plays a key role in neuroblastoma pathology, with implications for other *MYC*-driven cancers.

Abbreviations

ALA, alpha-linolenic acid (18:3ω3)
ALAM, alpha-linolenic acid metabolism
ARA, omega-6 arachidonic acid (20:4ω6)
DHA, omega-3 docosahexaenoic acid (22:6ω3)
DTrA, omega-9 docosatrienoic acid (22:3ω9)
EFAD, essential fatty acid deficiency
FA, fatty acids
FAS, fatty acid synthesis (pathways)
HUFA, highly unsaturated fatty acids, with 3 or more double bonds
LA, linoleic acid (18:2ω6)
LAM, linoleic acid metabolism
NB, neuroblastoma
NHF, normal human fibroblasts
OA, omega-9 oleic acid (18:1ω9)
TSmiRs, tumor suppressor microRNAs
UFAS, unsaturated fatty acid synthesis (pathways)
FAS, unsaturated and saturated fatty acid synthesis (pathways)
FAS-CG, FAS core genes (*FASN, ELOVL6, SCD, FADS2, FADS1*)
ω3, omega-3
ω6, omega-6
ω9, omega-9

INTRODUCTION

Neuroblastoma (NB) is a highly metastatic pediatric cancer derived from the neural crest-sympathoadrenal lineage that normally contributes to sympathetic ganglia, chromaffin cells of the adrenal medulla, and the paraganglia [1, 2]. *MYCN* is the defining oncogene of NB, where it was first discovered, receiving its *MYC-"N"* designation from NB itself [3, 4]. *MYCN* gene amplification is a hallmark of high-risk and poor prognosis disease. The MYCN and MYC transcription factors have highly overlapped function. MYC overexpression drives metabolic conversion to favor rapid generation of ATP via anaerobic glycolysis over oxidative phosphorylation, a shift known as the Warburg effect **(Figure 1a).** High lactate dehydrogenase (LDH), known to be transcriptionally regulated by MYC, is a hallmark of this effect shunting pyruvate use away from mitochondrial oxidative phosphorylation towards production and extracellular export of lactate [5]. The remaining pyruvate enters the mitochondria where it is converted ultimately to citrate and exported. Increased mitochondrial citrate efflux raises cytoplasmic citrate levels, where ACLY catalyzes release of acetyl-CoA, the fundamental building block for cytoplasmic *de novo* fatty acid synthesis (Figure 1b) [6]. MYC has been implicated in fatty acid (FA) synthesis (FAS) via glycolysis driven enhancement of acetyl-CoA production and increased expression of *de novo* FAS genes *ACLY*, *ACACA*, *FASN,* and *SCD* (Figure 1b) [7]. Similar to MYC, MYCN is associated with both enhanced glycolysis and metabolic reprogramming and has recently been implicated in fatty acid uptake and *de novo* synthesis in NB [8-11].

Apart from their role as an energy substrate, fatty acids are the main structural component of all cellular membranes. Specific non-esterified fatty acids are key to intracellular and paracrine cell signaling, as well as when acylated to phosphatidylinositol and diacylglycerol. Many paracrine (cell-cell) signals are immune-stimulating, including prostaglandins, 20-HETE, and leukotrienes

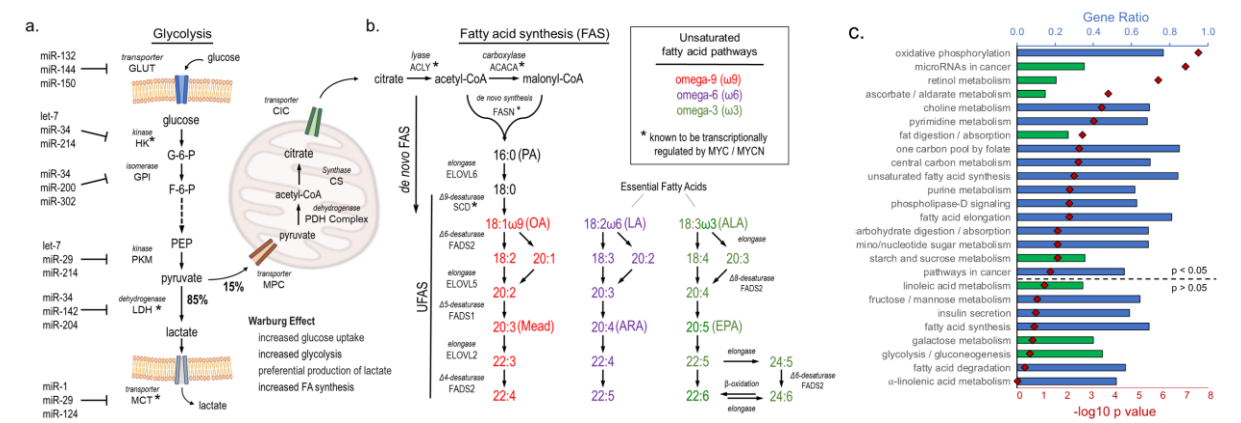

Figure 1. Biochemical pathways in glycolysis and fatty acid synthesis (FAS). a) Glycolysis with known suppression of genes by miRs. b) Fatty acid synthesis. FASN catalyzes *de novo* FA synthesis from excess citrate released by mitochondria with inhibited oxidative phosphorylation. Product 16:0 (palmitic acid, PA) enters elongation and desaturation pathways to yield oleic acid (18:1ω9) typically as a terminal product but can continue along a *de novo* pathway to at least a triene in the absence of sufficient highly unsaturated fatty acids (HUFA) to meet demand. Essential ω6 linoleic acid (18:2ω6, LA) and alpha linolenic acid (18:3ω3) are elongated and desaturated by the same set of enzymes. When cells cannot obtain LA or ALA, they desaturate and elongate 18:1ω9 to Mead acid (20:3ω9) and 22:3ω9). We define the unsaturated fatty acid synthesis (UFAS) genes as a subset of all fatty acid synthesis genes (FAS).

[12]. The relative proportions of the fatty acyl chains making up membrane phospholipids has a major influence on the signaling molecules produced on an 'as needed' basis in response to stimulation [13]. This constraint places extraordinary importance on the regulation of fatty acid derived signaling molecule production, which has implications for uptake, synthesis, downstream processing, and the relative proportion of individual fatty acids within cell membranes. With respect to cancer, fatty acid profiles can be an effect or a cause: transformation to malignancy alters the fatty acids of membranes, and fatty acid inputs are known to influence tumorigenesis [14-22].

Little is known about MYC or MYCN control downstream of *de novo* fatty acid synthesis (FAS), which usually terminates at monoenes, normally oleic acid, when sufficient polyunsaturates are available. Unsaturated fatty acid synthesis (UFAS), mediated by a subset of FAS genes (Figure 1b) is similarly little studied with respect to MYC and MYCN. UFAS modifies nascent and dietary fatty acids by both chain elongation and desaturation, the incorporation of double bonds at specific positions within the carbon chain [23]. Double bond distance from the terminal methyl group along with methylene-interruption between double bonds defines omega 3 (ω3), ω6, and ω9 unsaturated fatty acid classification (Figure 1b, Supplemental Figure 1a) [24]. Highly unsaturated FAs (HUFAs) such as ω6 arachidonic acid (ARA, 20:4) serve as substrates for numerous bioactive oxylipins, many of which are immune stimulating and pro-inflammatory [25, 26].

The HUFA ω3 docosahexaenoic acid (DHA, 22:6) is both critical to normal neuronal health and induces apoptosis in multiple cancer cell types [27-29]. FAS inhibition reduces NB cell line proliferation and xenograft growth [30]. *MYCN* has been implicated in fatty acid uptake [31, 32]. Seven isoforms of ELOVL genes code for enzymes that initiate fatty acid chain elongation, all of which exhibit chain length or double bond substrate specificity [33]. Among these, ELOVL4 initiates synthesis of very long chain HUFA (≥C26) and is highly expressed in retina and in differentiating neurons. MYCN represses *ELOVL4* in undifferentiated NB, making *ELOVL4* expression a marker of good prognosis and suggesting that FAS and metabolism may play an important role in NB pathogenesis [34].

MiRNAs are small, ~22 nucleotide long single stranded RNAs that repress translation through sequence-specific binding to the 3' untranslated regions (3'UTRs) of a wide range of target mRNAs. Altered miRNA function is central to NB development [12, 35-38]. Indeed, functional impairment of TSmiR *let*-7 is required for NB development [35]. Numerous additional NB-associated TSmiRs have been identified, including *miR-1*, *miR-22*, *miR-24*, *miR-34*, *miR-101*, *miR-124*, *miR-140*, *miR-150*, and *miR-204* [35, 39-49]. They play post-transcriptional regulatory roles in most cellular processes, including multiple metabolic processes such as regulation of glucose metabolism, obesity, and fatty acid oxidation by *let*-7, *mir*-22 and *miR*-33, respectively [50, 51]. *Let*-7 has been shown to target genes throughout the insulin-PI3K-mTOR pathway, including *IGF1R*, *INSR*, *IRS2* and *IGF2BP1*. Overexpression in mice also results in impaired glucose tolerance, demonstrating that miRNAs can regulate entire metabolic pathways *in vivo* through targeting of multiple pathway genes [51]. While many miRNAs have been implicated in a variety of metabolic processes throughout glycolysis (Figure 1a) [52, 53], their role in the UFAS pathways are largely unknown.

In this study, we set out to understand the expression patterns and outcome associations of FAS and UFAS in high-risk NB, as well as fatty acid levels *in vitro* in cell lines derived from high-risk NB. With complementary database searching and cultured NB cell measurements, we examined potential regulation of UFAS genes through MYCN and MYC activity and post-transcriptional regulation by TSmiRs. Finally, we profiled fatty acids levels of ω3, ω6, and ω9 unsaturated FAs in human NB cells. A consistent pattern emerged between high-risk NB outcomes, UFAS gene expression and regulation, and ω9 vs. ω3 and ω6 HUFA lipid profiles in NB. This model provides an organizing principle for future studies to fully understand how regulation of FAS and metabolism influences NB outcomes, with implications for other MYC family-driven cancers in general.

RESULTS

MYC and MYCN are both known to transcriptionally upregulate multiple genes contributing to the shift toward anaerobic glycolysis in high risk cancer, and multiple TSmiRs have been shown to post-transcriptionally regulate the relevant genes (Figure 1a). One of the results of this shift is the shunting of pyruvate towards lactate and citrate production, the latter of which contributes to elevated acetyl-CoA production, which is the fundamental building block of *de novo* FAS (Figure 1b). To investigate potential involvement of FAS and UFAS synthesis genes in NB, we performed KEGG pathway analysis of metabolic pathways in high-risk vs. low-risk NB patients. We observed a significant enrichment of the UFAS pathway in high-risk disease, whereas the *de novo* FAS pathway was not significantly elevated (Figure 1c). Heatmap analysis of the genes in these two KEGG pathways show a highly enriched gene cluster of UFAS genes *SCD*, *FADS2*, and *FADS1* as well as the FAS genes *FASN and ELOVL6*, in high-risk patients (**Figure 2**). These genes make up most of the FAS genes outlined in the parallel fatty acid metabolism pathways (*Figure 1b*), suggesting that these genes may make up an important genetic circuit in high-risk disease.
We next analyzed the expression of FAS pathway genes (Figure 1b) *ACACA*, *FASN*, *ELOVL6*, *SCD*, *FADS2*, *ELOVL5*, *FADS1*, and *ELOVL2* in low-risk vs. high-risk NB patients. Of these genes, all were significantly upregulated in high-risk patients except *ACACA*, *ELOVL5*, and

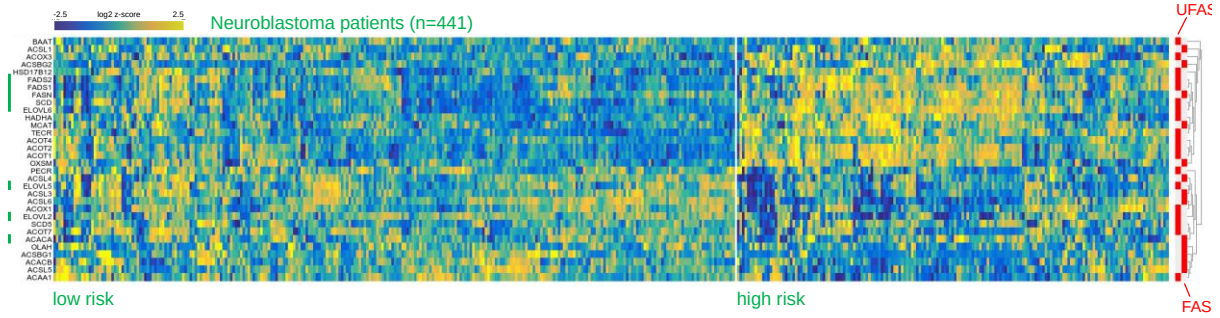

Figure 2. KEGG pathway cluster analysis of neuroblastoma patients. Heatmap of *unsaturated* fatty acid synthesis (UFAS) and fatty acid synthesis (FAS) pathway gene expression in stage 1-4 neuroblastoma patients, comparing low-risk (*n=270*) and high-risk disease (*n=171*). FAS and UFAS pathway genes from *figure 1b* are highlighted by vertical green bars on left. Genes associated with UFAS and FAS gene sets are identified by clustered red bars on right. Expression data presented as normalized values (log2 z-scores).

ELOVL2 (**Figure 3a**). The upregulated genes were also strongly associated with poor prognosis in NB patients, whereas *ACACA* and *ELOVL5* were not associated. *ELOVL2* was unique among the gene set in that high expression was associated with improved prognosis (Figure 3b). We also examined expression patterns of this gene set in eight human NB cell lines cultured in our laboratory using RNA sequencing (RNA-Seq) analysis and observed that these genes are similarly upregulated compared to normal human fibroblasts (NHF) (Supplemental Figure 2, Figure 3c). *ACACA* was elevated in NB cells vs. NHF, suggesting that *ACACA* may be generally unregulated in NB over normal tissues if not further enriched in high-risk disease. *ELOVL5* was largely unchanged and *ELOVL2* expression was very low in general, which is generally consistent with human patient expression and overall survival data (Figure 3a, 3b, 3c). The patterns of expression and prognostic association of these genes in both patients and cell lines strongly suggest that UFAS synthesis and metabolism plays an important role in the pathology of high-risk and poor prognosis NB. These observations further establish that FAS pathway genes *FASN*, *ELOVL6*, *SCD*, *FADS2*, *FADS1* represent a "core" prognostic gene (FAS-CG) set for *de novo* synthesis of ω9 fatty acids and metabolic processing of ω3 and ω6 fatty acids that are uniformly elevated in NB and enriched in high-risk, poor prognosis disease.

Glycolysis is a highly regulated metabolic process, controlled by energy needs, glucose availability, and cell state [54]. Conversion from oxidative phosphorylation towards anaerobic glycolysis is common in cancer. Broad post-transcriptional regulation of glycolysis pathway genes by multiple TSmiRs is consistent with this conversion. While in normal tissues and cells, relatively high levels of TSmiRs contribute to glycolysis modulation, resulting in a typical 1:9 ratio of ATP

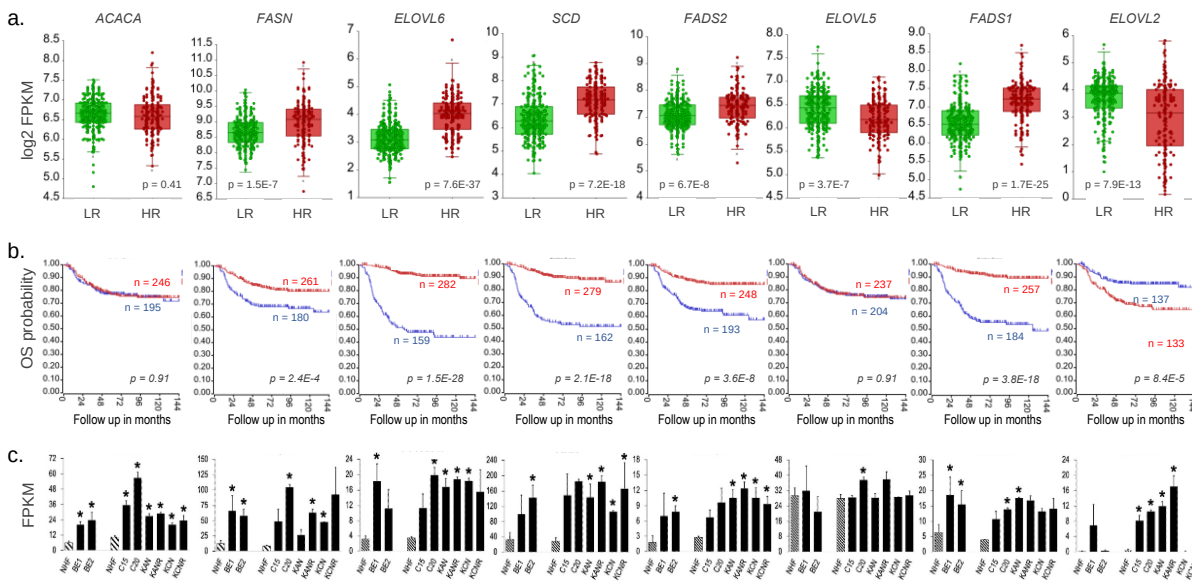

Figure 3. U/FAS genes are elevated in high-risk neuroblastoma and associate with poor prognosis. a) Gene expression levels in human NB patients with low-risk (LR, n = 270) or high-risk (HR, n = 171) disease. **b)** Overall survival (OS) in stage 1-4 neuroblastoma patients by gene expression. High / low cutoff is average expression. **c)** Expression levels of UFAS genes in normal human fibroblasts (NHF) and human neuroblastoma cell lines (left set of NHF and BE1, BE2 NB cell lines represents n = 3 sequencing rounds; right set of NHF and NB cell lines represents n = 2 sequencing rounds *p<0.05).

production between glycolysis and oxidative phosphorylation. In cancer, many of the TSmiRs that negatively regulate glycolysis genes are themselves impaired or downregulated, contributing to release of most glycolysis genes from normal post-transcriptional inhibition, significantly contributing to a cancer associated shift away from oxidative phosphorylation-based ATP production, which results in an increased 6:4 ratio of ATP production through glycolytic mechanisms. Given the importance of glycolysis regulation and the degree to which TSmiRs play an important role in regulation of the pathway and our newly discovered role for FAS and UFAS in NB outcomes, we hypothesized that TSmiRs might similarly target FAS and UFAS pathway genes. There are multiple known NB TSmiRs, including *miR-1*, *let-7*, *miR-22*, *miR-24*, *miR-34*, *miR-101*, *miR-124*, *miR-140*, *miR-150*, and *miR-204* [55, 56]. We analyzed the 3'UTRs of the U/FAS-CGs for presence of binding sites for this NB TSmiR list and discovered widespread target-site presence among all U/FAS-CGs, with an average of 12.2 TSmiR sites per 3'UTR. (Table 1). Even the 3'UTRs of FAS genes not associated with poor prognosis (*ACACA*, *ELOVL5*, and *ELOVL2*) are highly enriched with TSmiR sites (average of 11 sites per 3' UTR), suggesting a unified post-transcriptional regulation of FAS pathways by TSmiRs in normal biology and in cancer. MYCN is regulated by TSmiRs in NB and serves here as a positive control. The *MYCN* 3'UTR contains eight TSmiR sites as well, despite its relatively small size. As a control, housekeeping genes *SDHA*, *HPRT1*, *ACTB*, and *GAPDH* have minimal TSmiR sites by comparison, with an average of only one site per 3' UTR. Two non-FAS related genes, *IGTAV* and *DLK1*, both with long 3' UTRs have only two identified TSmiR sites per mRNA. Together these ratios of TSmiR sites suggest broad post-transcriptional regulation of the FAS pathways by TSmiRs, similar to what has been reported in glycolysis. Further, several NB related TSmiRs, *miR-1*, *let-7*, *miR-34*, *miR-124*, and *miR-204*, have been linked to glycolysis gene regulation as well (Figure 1a), suggesting that a large TSmiR "super" regulatory network may influence both glycolysis and FAS and is consistent with a model where glycolysis and FAS may be co-elevated in cancer, including high-risk NB.

The TSmiRs assessed here have each been previously demonstrated to possess anti-growth tumor suppressor function and frequently reduced expression in NB [44, 45]. We observed that the entire TSmiR set was uniformly downregulated in tyrosine hydrolase-MYCN (*TH-MYCN)* driven murine NB compared to the sympathetic ganglia tissue of origin, demonstrating broad inhibition of multiple TSmiRs during NB development and collectively confirming the previous single-TSmiR reports of impaired function in NB (**Figure 4**). The oncogenic *miR-17-92* cluster (which includes miRNAs *miR-17*, *miR-18a*, *miR-19a, miR-19b*, *miR-20a*, and *miR-92a*) is a known transcriptional target of MYCN and is upregulated in *TH-MYCN* tumors, as expected. MiRNAs affect their mRNA targets by one or more of three main mechanisms: translation inhibition, mRNA sequestration and storage, and mRNA degradation. A recent meta-analysis of miRNA inhibition mechanisms revealed that half of all miRNA target genes are regulated primarily through varying degrees of mRNA decay [57].

We thus reasoned that mRNA levels of some or all of the FAS TSmiR target genes may be reduced by elevated TSmiR activity and therefore examined the effects of TSmiR overexpression on *miR-22*, *let-7*, and *miR-124* targeted FAS mRNA levels in existing TSmiR overexpression

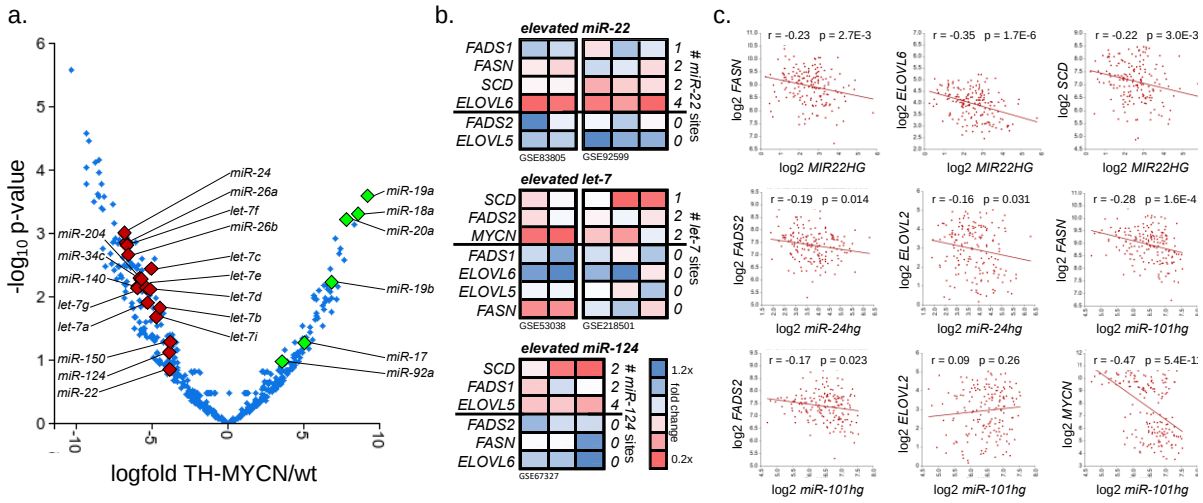

Figure 4. Tumor suppressor miRNAs are downregulated in TH-MYCN neuroblastoma and result in reduced expression of their U/FAS mRNA targets. a) Volcano plot of differentially expressed miRNAs in *TH-MYCN* neuroblastoma tumors (n = 12) and sympathetic ganglia (n = 12, neuroblastoma tissue-of-origin). The y-axis indicates -log 10 p-values; x-axis indicates log2 fold change (FC) between tumors and ganglia. Red diamonds: tumor suppressor miRNAs from *Table 1*; green diamonds: miRNAs of the miR-17-92 oncomiR cluster. **b)** Heatmaps of U/FAS genes expression changes in response to *miR-22* (top), *let-7* (middle), or *miR-124* (bottom) overexpression. Each study is a separate heat map box with the GSE# listed below. Each column represents a replicate experiment. **c)** Correlation plots for miRNA-host gene vs. mRNA-target gene expression for *miR-22*, *miR-24*, and *miR-101* in n = 176 high-risk neuroblastoma patients.

datasets (supplemental Figure 3). Fold-change heatmaps of two independent *miR-22* overexpression studies displayed similar patterns of reduced expression of m*iR-22* targets *FADS1*, *FASN*, *SCD*, and *ELOVL6,* which contains four miR-22 sites in its 3' UTR (**Table 1**) and was strongly suppressed in both studies. In contrast, expression levels of both *FADS2* and *ELOVL5*, which is not targeted by *miR-22*, were not affected (Figure 4b, top panels). A similar pattern of reduced expression was observed for *let-7* targets *SCD*, *FADS2*, and *MYCN* in studies of de-repressed l*et-7* biogenesis and *let-7* transfection. Levels of non-*let-7* targets *FADS1*, *ELOVL6*, and *ELOVL5* were relatively unaffected, whereas non-*let-7* target *FASN* levels were reduced in the *let-7* biogenesis study, but minimally effected by transfected *let-7* (Table 1; Figure 4b, left and right middle panels, respectively). *MiR-124* transfection resulted in reduction of miR-124 targets *SCD*, *FADS1*, and *ELOVL5*, whereas none of non-miR-124 targets *FADS2*, *FASN*, and *ELOVL6* were decreased (Table 1; Figure 4b, lower panel).

Many genomic miRNA loci are located within introns of larger host genes and are coordinately transcribed as part of the host transcript from which they are then processed. Expression levels of a miRNA and its host-gene are therefore often correlated, as with *miR-22* and *miR-24* expression, which are strongly associated with their respective host genes *MIR22HG* and *C9orf3* [58-60]. Host gene miRNA gene expression patterns thus serve as a proxy for intergenic miRNA expression levels located within the primary transcript. We therefore compared expression levels of each of the *miR-22*, *miR-24*, and *miR-101* host genes (*MIR22HG*, *C9orf3*, and *JAK1*, respectively) to the expression levels of individual *miR-22* targets *FASN*, *SCD,* and *ELOVL6*, *miR-*

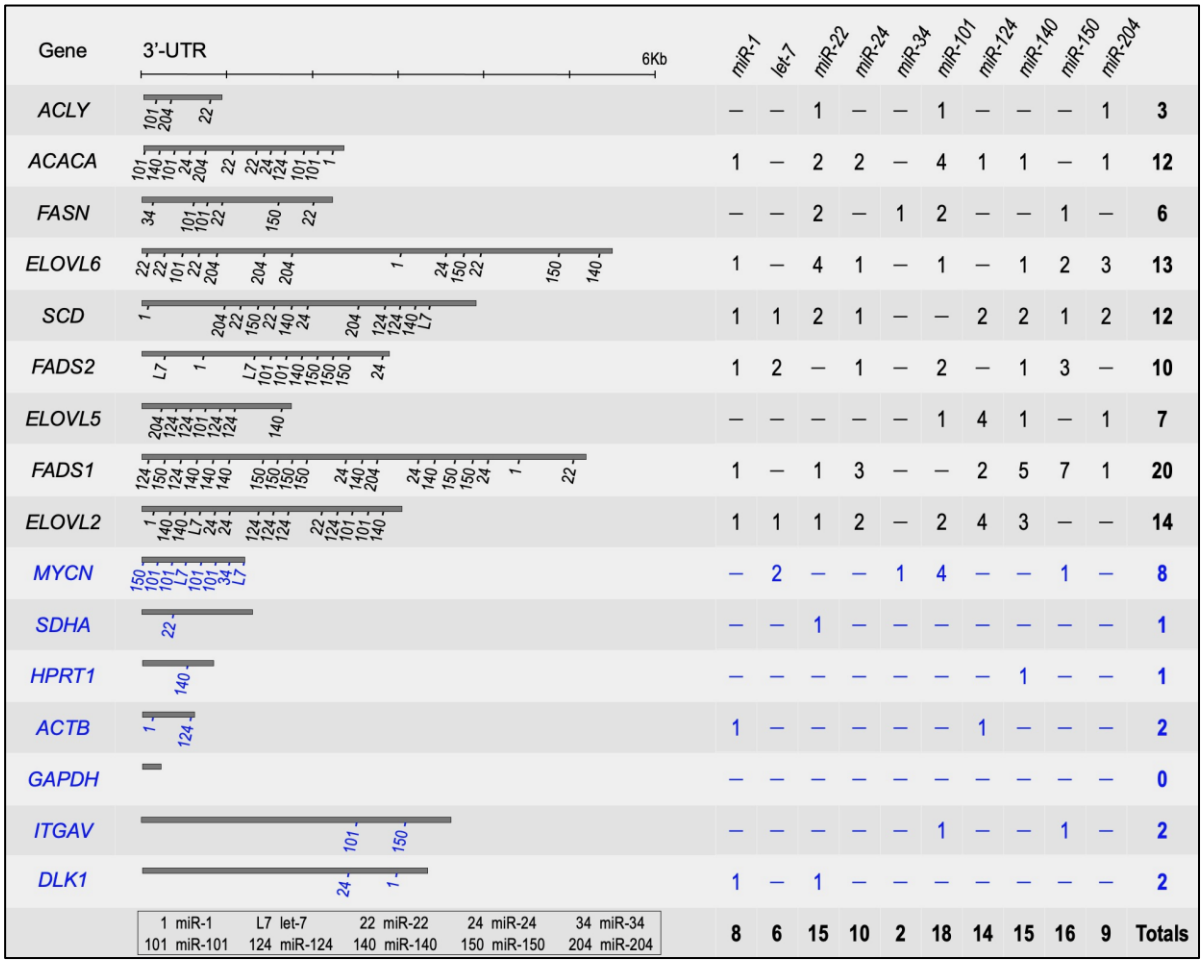

Table 1. FAS-UFAS gene 3' UTRs showing position of predicted microRNA target sites. The table shows a count of sites in multiple U/FAS genes along *MYCN* as a positive control UTR and several housekeeping genes (*SDHA*, *HPRT1, ACTB*, and *GAPDH*) and two unrelated genes (*ITGAV* and *DLK1*).

24 targets *FADS2* and *ELOVL2*, and *miR-101* targets *FASN*, *FADS2*, *ELOVL2*, and *MYCN* (Figure 4c). All three *miR-22* and both *miR-24* target genes are inversely correlated with miRNA host gene expression. *FASN*, *FADS2* and *MYCN* are inversely correlated with *miR-101* hg expression, whereas *ELOVL2* expression is not significantly associated. These expression patterns provide further support for a model where U/FAS genes are broadly targeted by TSmiR in NB. While these results are consistent with TSmiR targeting of FAS genes, further work will be required to validate these observations.

MYC overexpression drives metabolic conversion to favor rapid generation of ATP via anaerobic glycolysis over oxidative phosphorylation; *MYCN* is similarly associated with enhanced glycolysis and metabolic reprogramming in NB [8-10]. Given the predominance of MYCN activity in poor prognosis NB and the existing strong connection of the *MYC* family with metabolic reprogramming, we hypothesized that *MYC* and *MYCN* would also influence FAS gene expression. We therefore analyzed FAS gene expression in complimentary datasets of induced *MYC* expression in P493-6 lymphoid cells and JQ-1 bromodomain inhibitor mediated MYCN inhibition in BE(2)C NB cells (**Figure 5a**, 5b). As previously shown, MYC induction resulted in

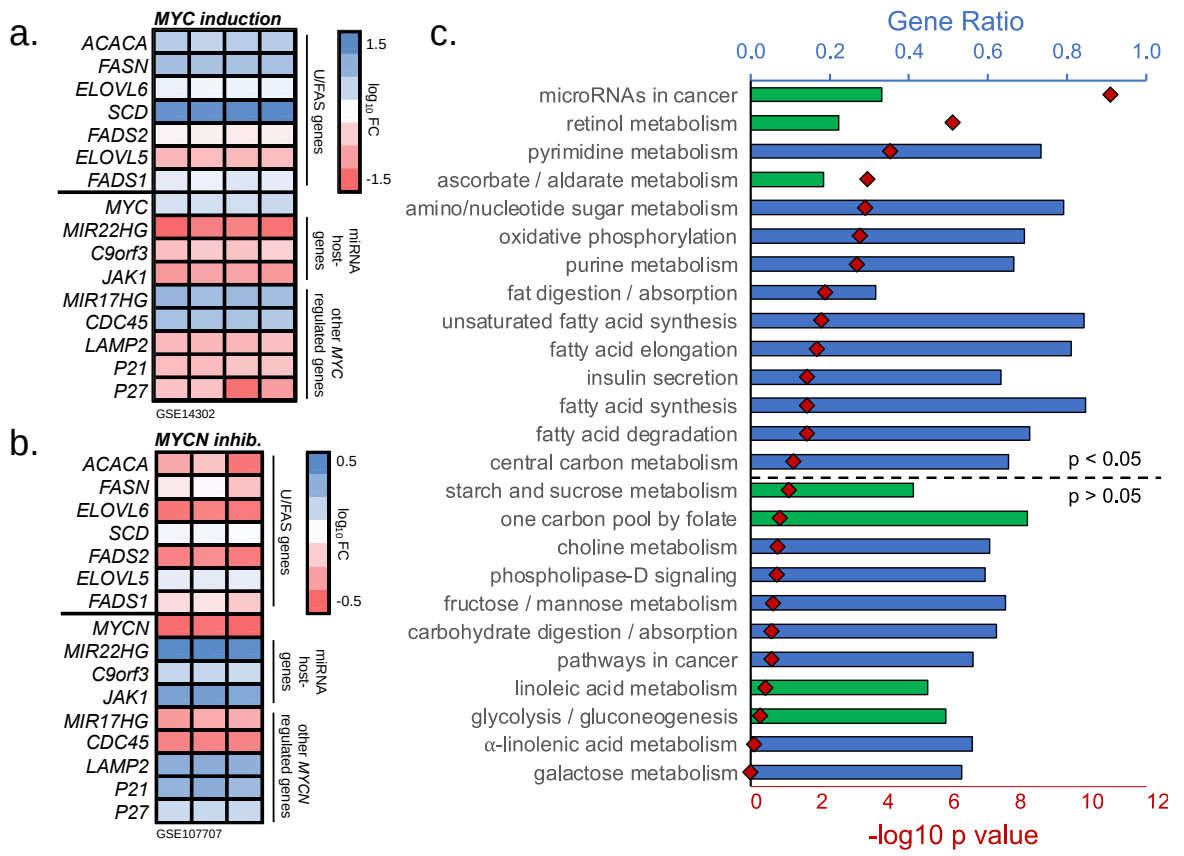

Figure 5. Expression patterns in neuroblastoma by KEGG Gene Set Analysis. a) Heatmaps of MYC induction or b) MYCN inhibition by JQ-1 bromo-domain inhibitor for FAS and MYC or MYCN target gene expression. Each study is a separate heat map box with the GSE#. Each column represents a replicate experiment. **c)** KEGG pathway analysis of altered metabolic or cancer related pathways in high-risk (n = 171) *vs*. low-risk (n = 270) neuroblastoma patients. Blue bars = overrepresented pathways; green bars = underrepresented pathways; red diamonds = -log10 p values.

significant upregulation of U/FAS genes *ACACA* (6.6x), *FASN* (9.2x), and *SCD* (33.2x), and *ELOVL6* (2.6x). *FADS2*, *ELOVL5*, and *FADS1* expression were also significantly increased 2.6x, 1.6x, and 3.1x, respectively. Known MYC activated (*MIR17HG* and *CDC45*) and suppressed (*LAMP2*, *P21*, and *P27*) genes behaved as expected (Figure 5a). In BE(2)C cells treated with the MYCN inhibitor JQ-1, FAS genes were consequently downregulated between 0.4x and 0.67x (Figure 5b). *FADS2* and *ELOVL6* were the most affected genes, with expression decreased to 33% of control in both cases. MYC family targets genes once again behaved as expected, with decreased *MIR17HG* and *CDC45* levels and de-repressed *LAMP2* and *P21* expression.

These data suggest that MYC and MYCN broadly regulate the FAS pathways, identifying novel roles for MYC and MYCN transactivation of *FADS2* and *FADS1*, with *ELOVL6* being an additional novel target of MYCN. Further, in KEGG analysis of *MYCN* amplified vs. *MYCN* non-amplified human NB patients, several fatty acid pathways are significantly enriched in the *MYCN* amplified group (Figure 5c). Whereas high-risk NB patients (where many but not all are *MYCN*-amplified)

have a significantly enriched FAS pathway, *MYCN*-amplified patients, where *MYCN* is highly expressed, KEGG pathways for FAS, fatty acid elongation, fat digestion / absorption, and fatty acid degradation are all significantly elevated, strongly suggesting that MYCN is a master regulator of fatty acid metabolism in NB. MiRNA host genes *MIR22HG*, *C9orf3*, and *JAK1* are all responsive to MYC and MYCN modulation as well, being upregulated by *MYC* activation and suppressed upon MYCN inhibition (Figure 5a, 5b), providing a possible mechanism for TSmiR suppression in NB and other MYC-driven cancers. It is also possible that FAS gene expression levels in cancer are in part regulated indirectly by MYC and MYCN through transcriptional suppression of TSmiR host gene expression and consequent release of FAS mRNAs from post-transcriptional degradation by the embedded TSmiRs. Such a model would establish a regulatory network between MYC/MYCN, FAS genes, and TSmiRs (which also target *MYCN* mRNA in NB).

We next consider fatty acid profiles in eight NB cell lines analyzed with gas chromatography and mass spectrometry (**Figure 6a**, Supplemental Figure 1b, 2). ω9 Mead acid and elongation product docosatrienoic acid (DTrA) were dramatically increased many fold beyond levels seen in normal cells and fluids (Figure 6a, Supplemental Figure 3). NHF cells have a higher proportion of DHA than all NB cells. Elevated Mead acid, normalized to arachidonic acid, known as the triene/tetraene ratio (T/T), is the accepted index of essential fatty acid deficiency (EFAD). In plasma, a T/T greater than 0.4 indicates EFAD; a similar threshold applies to cells [61]. In NB cell lines, ARA levels fell from 10% w/w in NHF to ~5% w/w while Mead acid increased from trace levels to 2% - 5% of total fatty acids (Figure 6a, Supplemental Figure 4a), reflecting EFAD for all cells. The sum of Mead acid and ARA is 8.8%±1.2%,w/w (mean ± SD) reflecting the compensatory

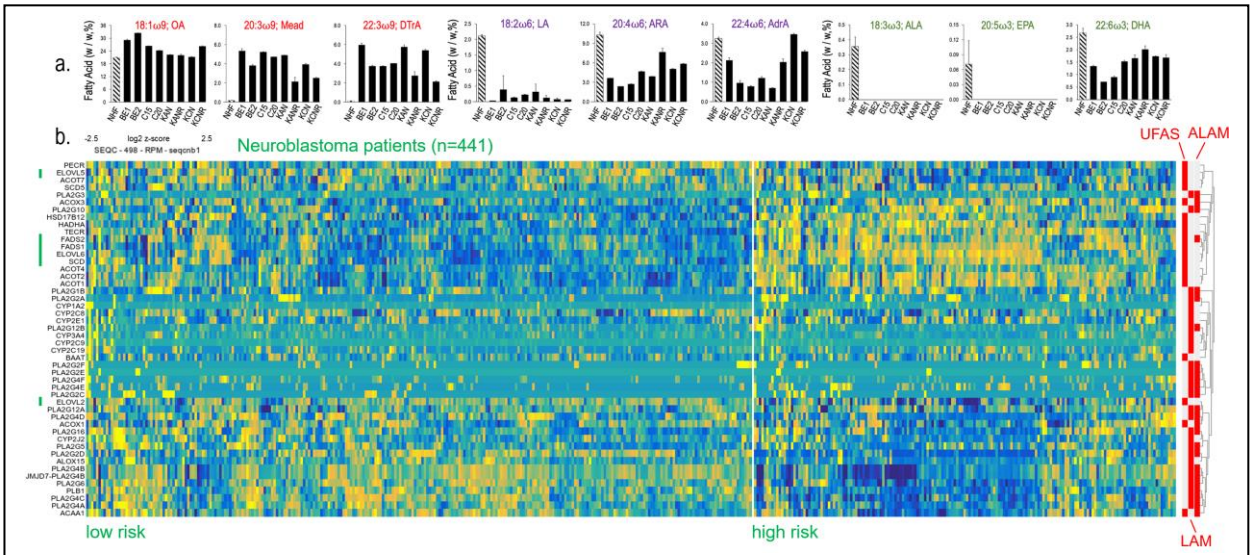

Figure 6. Omega-9 unsaturated fatty acids are elevated in neuroblastoma. a) Fatty acid levels in normal human fibroblasts (NHF) and human neuroblastoma cell lines, presented as percent of overall lipid weight (w/w %). Omega-9 fatty acids are titled in red, omega-6 are titled in purple, and omega-3 are titled in green. **b)** Heatmap of *unsaturated* fatty acid synthesis (UFAS), linoleic acid metabolism (LAM), and α-linolenic acid metabolism (ALAM) gene expression in stage 1-4 neuroblastoma patients, comparing low-risk (n = 270) and high-risk disease (n = 171). FAS and UFAS pathway genes from *figure 1b* are highlighted by vertical green bars on left. Genes associated with UFAS gene sets are identified by clustered red bars on right. Expression data presented as normalized values (log2 z-scores).

increase in Mead acid levels as ARA decreases [61] (Supplemental Figure 4c, 4d). Normally, EFAD arises because of restricted supply of ω6 LA (Figure 1b, Supplemental Figure 1) [62]. However, NHF grown in the same media as the NB cells had trace Mead acid and thus was not EFAD. The enhanced expression of UFAS genes compared to NHF cells points (Figure 3c) as well as the pattern of fatty acid levels, discussed below, points to unusually high synthesis of HUFA, and possibly Mead acid specifically.

KEGG pathway analysis of UFAS pathways in low-risk *vs*. high-risk NB patients revealed that while the *de novo* FAS pathway genes are uniquely enriched in high-risk patients, the majority of ω3 precursor ALA and ω6 precursor LA metabolism genes represented by UFAS are suppressed. In contrast, genes from the three pathways are largely uniformly expressed in both normal adrenal gland and tibial nerve tissue samples (Figure 6b, Supplemental Figure 5), together suggesting that a genetic program favoring *de novo* FAS over UFAS may be selected in high-risk NB.

Derivatives of ω6 ARA are produced along three main pathways driven by lipoxygenases (i.e., ALOX5), cyclooxygenases (i.e COX2) or CYP450 enzymes [12]. Out of the more than 50 unique CYP450 enzymes, 15 are epoxygenases that act on HUFAs like ARA. Only two of these 15 are expressed in NB; *CYP2C8* and *CYP4V2* (Supplemental Figure 6). ARA processing by these enzymatic arms produces several pro-inflammatory eicosanoids, among which are prostaglandins, thromboxanes, leukotrienes, DHET, and 20-HETE. These eicosanoids can stimulate immune activity, and have been involved in tumor formation and progression, where *ALOX5* has been implicated as a tumor suppressor [63]. The enzymes along these ARA processing arms of these pro-inflammatory eicosanoids are uniformly downregulated in high-risk NB (Supplemental Figure 7). Indeed, low expression of this gene set is strongly associated with poor prognosis (Supplemental Figure 8), together suggesting a selective advantage for reduced ω6 levels in NB, which is consistent with what we observe in NB cell lines.

DISCUSSION

MYC, *MYCN*, and numerous TSmiRs have been implicated throughout the glucose metabolism pathway. We have shown here that the *MYCN*/TSmiR regulatory program is similarly involved in FAS pathway regulation in NB with elevated expression of FAS-CG in high-risk disease that strongly associate with poor prognosis (Figure 1-3). The remarkably high ω9 HUFA Mead acid and DtrA levels in cultured NB cells and concordant gene expression data between cells and NB patients suggest that the upstream FAS pathway consisting of FASN and ELOVL6 can serve as a de facto UFAS pathway for the specific production of ω9 fatty acids. Careful inspection of the ω3 fatty acids show that only terminal ω3 DHA is present at an appreciable concentration, with precursor ALA and intermediate ω3 EPA at trace levels (Figure 6a). Similarly, for ω6 fatty acids, ω6 precursor LA is low in all cells, while the usual terminal product ω6 ARA and its elongation product ω6 AdrA are present. Indeed, there is some indication that ω9 OA may be elevated beyond its already dominant level in some NB cell types. Upregulation of the UFAS genes and the upstream pathway may induce an apparent essential fatty acid deficiency via usually high production of Mead acid.

We propose a model where *MYCN* and TSmiRs oppositely regulate FAS in NB as a continuation of the well-established Warburg effect that shunts ATP production from oxidative phosphorylation towards glycolysis, which connects directly to UFAS through increased production of acetyl-CoA, the fundamental building block of *de novo* FAS. This model introduces UFAS genes *ELOLV6*, *FADS2*, and *FADS1* as novel targets of MYCN in NB and broad collective post-transcriptional regulation of FAS and UFAS genes by multiple TSmiRS. This model has implications for MYC family driven cancers in general, in part due to the highly overlapped effects of MYC and MYCN on U/FAS genes and TSmiR host gene transcription (Figure 5).

While reports of ω9 Mead acid in cancer are generally scarce, it was shown to be elevated in both the serum and tumors of 38% of hepatocellular carcinoma patients. It was not present in other tissues, suggesting that Mead production was elevated only in the tumor itself [21]. Mead acid treatment increased proliferation of HRT-18 breast cancer cells whereas ω3 EPA (Figure 1b, Supplemental Figure 1b) reduced cell growth [64]. Further, Mead acid increased both invasion activity and cell growth of multiple squamous cell cancer lines [65]. Together these studies suggest that Mead acid may provide a growth advantage in cancer, which could partially explain the elevated ω9 Mead acid production we see in NB cells.

FADS2 dysregulation at the 11q13 major cancer hotspot region alters fatty acid metabolism in several cancer types [66]. FADS2 activity is promiscuous, it operates on at least 16 substrates catalyzing biosynthesis of several unsaturated fatty acids by Δ6, Δ8, and Δ4 desaturation [23]. The availability of fatty acid substrates to FADS2 in any tissue is the major determinant of the final product mixture for further membrane lipid synthesis and/or synthesis of signaling molecules [67-69]. *FASN*, *ELOVL6*, and *SCD* are the classical *de novo* FAS pathway and produce ω9 oleic acid (OA)(Figure 1b, 3a). These three genes are also among the most upregulated of the FAS-CG group, consistent with high OA production. Indeed, the actual amount of OA produced is likely even higher given that OA is further processed to downstream ω9 fatty acids (Figure 6).

Our observations outline a possible genetic disposition towards lowering ω6 and ω3 fatty acid metabolism in high-risk NB. Genes from the LA (ω6) and ALA (ω3) metabolism pathways are downregulated in high-risk disease compared to the UFAS-CGs (*FASN*, *ELOVL6*, *SCD*, *FADS2*, and *FADS1*), which are significantly enriched in high-risk over low-risk and in *MYCN* amplified over *MYCN* non-amplified NB (Figure 2, 6b). The FADS2 and FADS1 desaturases introduce double bonds into ω3, ω6, and ω9 fatty acid chains. They have highest affinity for ω3 fatty acids, followed by ω6 and then ω9, and yet ω9 fatty acids were enriched in NB cells. Cellular ω3 ALA and ω6 LA precursors are depleted to trace levels, thus unmasking *de novo* synthesis of Mead acid and DtrA. Production of Mead acid and DTrA in NB may well be driven by significantly increased ω9 substrate availability as well as upregulated UFAS. FASN, ELOVL6, and SCD complete *de novo* FAS and produce oleic acid (OA), the first ω9 fatty acid in the ω9 pathway (Figure 1b, 3a). These three genes are also among the most upregulated of the UFAS-CG group, suggesting that flux through OA production may be high. Indeed, OA quantities in many NB cells are higher than in NHF, and in all cases but the actual amount of OA produced is almost certainly even higher given that OA is further processed to the elevated levels of downstream ω9 unsaturated fatty acids (Figure 6).

Selective pressures may also explain the elevated ω9 and decreased ω3 and ω6 levels we observe in NB (Figure 6). Multiple studies have shown ω3 HUFA EPA and in particular DHA have anti-cancer activity through induction of apoptosis in multiple cancers [28]. DHA treatment of ovarian and lung cancer cell lines and an *in vivo* mouse model of ovarian cancer increased ROS production and induced apoptosis *in vitro* and reduced tumor Ki67 staining and tumor size *in vivo* [70, 71]. Interestingly, pretreatment with the antioxidant NAC reversed these effects, suggesting that ROS production may be a key mechanism of growth inhibition by DHA. DHA and other HUFAs are known to be highly sensitive to ROS which attacks double bonds in the fatty acid chains. ROS/HUFA reaction produce hydroperoxides on the fatty acid chains, resulting in chain reactions that further propagate ROS production and damage. These observations collectively provide support for selective pressure to suppress ω3 synthesis in NB.

Chronic inflammation is associated with increased cancer incidence, whereas an inflammatory tumor microenvironment and acute inflammation have been shown to increase anti-cancer immune function and immune therapy efficacy [72]. Local inflammation is also linked to immune cell infiltration. While some adult tumors, like melanoma, are considered “hot” tumors with high local inflammation and immune cell presence, pediatric solid tumors are most often “cold” [73]. NB is a classically cold tumor. In fact, NB was recently reported to have the lowest inflammation response signature of 37 tumor types, demonstrating that NB has strongly suppressed inflammatory signaling. *MYCN* amplification was shown to reduce inflammatory signaling even further, which is consistent with the limited efficacy of immune therapies in NB [74].

Our observations surrounding ω6 fatty acids provide a plausible explanation for a reduced inflammatory signature in NB. Both LA and ARA serve as key precursors for pro-inflammatory eicosanoids [12]. Lower levels of both LA in ARA in NB reduce the pool of precursors available to produce them. Moreover, we observed reduced expression of all three (*ALOX5*, *CYP450*, and *COX*) enzyme pathways that produce inflammatory eicosanoids from ARA in high-risk NB (Supplemental Figure 7). Low expression of these genes is also strongly associated with worse prognosis (Supplemental Figure 8). Our observations are consistent with the low inflammatory signature of NB, providing a potential mechanism through metabolic reprogramming that favors ω9 fatty acid production over ω6 ARA. Furthermore, recent studies have also demonstrated a pro-apoptotic effect for ARA on cancer cells and revealed anti-tumor effects of ARA metabolism, providing further support for a selective pressure to minimize both ARA and downstream eicosanoid production [75-78].

We show here that unsaturated fatty acid synthesis is deregulated in high-risk NB by both MYCN activity and TSmiR disruption and contributes to poor outcomes. We also report altered lipid profiles in NB cells through decreased ω3 and ω6 and increased ω9 fatty acid levels, which may be selected to minimize ω3-driven ROS toxicity and ω6-driven pro-inflammatory signaling. Our results reveal a unified metabolic reprogramming of fatty acid synthesis that has similarities to *MYC* and TSmiR regulation of glycolysis, with implications for *MYC* family-driven cancers,

suppression of inflammation in cold tumors, and new opportunities for therapies that modulate unsaturated fatty acid dietary intake and synthesis.

MATERIALS AND METHODS

R2 database: Human NB patient RNA-seq expression and overall survival data sets were obtained from the R2: microarray analysis and visualization platform (http:// r2.amc.nl) [64]. Data sets used: SEQC-498; An Investigation of Biomarkers Derived from Legacy Microarray Data for Their Utility in the RNA-Seq Era, GEO accession number GSE62564 [65], Ghent-24; The role of miRNAs in NB tumor development, r2 dataset identifier E-MTAB-2618. Expression graphs, Kaplan-Meier curves, and KEGG pathway analysis was performed using data analysis tool suite on the r2 database web portal.

Cell Lines: All NB cell lines were obtained from the Childhood Cancer Repository at the Texas Tech University Health Science Center, which is part of the Children's Oncology Group. BJ-1 normal human fibroblasts were purchased from ATCC. All cells were grown in RPMI-1640 media supplemented with 10% fetal bovine serum.

RNASeq: Total RNA was submitted for library prep and sequencing to LC Sciences (Houston, TX). For the present research, we are reporting UFAS genes and will report out other genes elsewhere. RNA-seq data sets are available under GEO reference series GSE(TBD) (http://www.ncbi.nlm.nih.gov/geo/query/acc.cgi?acc=GSE(TBD)).

Two batches of NB cell lines (black columns) were submitted for RNA-Seq analysis; Batch 1: NHF, BE1, and BE2 (n = 3 replicates per cell line), Batch 2: NHF, CHLA15, CHLA20, KAN, KANR, KCN, KCNR (n = 2 replicates per cell line). Bars represent the mean fragments per kilobase of exon per million mapped fragments (FPKM) of either three or two independent experiments for Batch 1 and Batch 2, respectively. The error bars represent the standard deviation. For each gene expression graph, expression values for individual NB cell lines (black columns) were compared to Batch- specific NHF cell expression (black and white stripped columns). Due to the small sample sizes (n = 3 or n= 2), an initial f-test was used to determine if a student's t-test or Welch's t-test should be employed. A* denotes a $p < 0.05$.

MicroRNA target site identification: Predicted miRNA target sites were identified for each gene using TargetScan version 8.0 (https://www.targetscan.org/vert_80/) [70, 71]. Briefly, 3' UTRs were matched to predicted binding of TSmiRs known to be associated with NB, specifically *miR-1*, *let-7*, *miR-22*, *miR-26*, *miR-34*, *miR-142*, *miR-150* and *miR-204*.

Existing datasets used for TSmiR and *MYC*/*MYCN* modulation response: Five published datasets were used to analyze UFAS gene expression changes in response to TSmiR modulation: GSE83805: doxycycline induced *miR-22* expression in RD18 rhabdomyosarcoma cells (n = 2 independent experiments), GSE92599: *miR-22* transfection in 293T human embryonic kidney cells (n = 3 independent experiments), GSE53038: *LIN28A* knockdown in H9 human embryonic stem cells. The LIN28 family is a strong repressor of *let-7* biogenesis [35]. Inhibiting LIN28A

results in a significant increase of *let-7* family members [79] (n = 2 independent experiments), GSE218501: *let-7* transfection in human dermal lymphatic endothelial cells (n = 3 independent experiments), GSE67327: PEO1 *miR-124* transfection of PEO1 ovarian cancer cells (n = 3 independent experiments). GSE14302: tetracycline "off" *MYC* induction in P493-6 human EBV-transformed B lymphocytes (n = 4 independent experiments), GSE107707: MYCN inhibition by the JQ-1 bromodomain inhibitor in BE(2)C NB cells (n = 3 independent experiments). Heatmaps were generated by determining expression levels in response to TSmiR expression, *MYC* induction, or MYCN inhibition, relative to untreated controls in each dataset. Each heatmap box represents fold change of one replicate within the study.

Fatty Acid Profiling: Fatty acid analysis of cultured cells was performed as described previously [69, 80-82]. Briefly, cells pellets are harvested after centrifugation and fatty acid methyl esters (FAME) are prepared according to a modified one-step method [83]. FAME were structurally identified by gas chromatography (GC) - chemical ionization mass spectrometry (GC/CI-MS/MS) [84, 85] and quantified by GC-flame ionization detector (GC-FID) after calibration with an equal weight FAME standard mixture to develop response factors.

Acknowledgement. This work was supported by a research award (to JTP) from Cancer Prevention and Research Institute of Texas (CPRIT).

References

1. Aminzadeh, S., et al., *Energy metabolism in neuroblastoma and Wilms tumor.* Transl Pediatr, 2015. **4**(1): p. 20-32.
2. Raieli, S., et al., *MYCN Drives a Tumor Immunosuppressive Environment Which Impacts Survival in Neuroblastoma.* Front Oncol, 2021. **11**: p. 625207.
3. Kawada, K., M. Iwamoto, and Y. Sakai, *Mechanisms underlying (18)F-fluorodeoxyglucose accumulation in colorectal cancer.* World J Radiol, 2016. **8**(11): p. 880-886.
4. Zimmerman, M.W., et al., *MYC Drives a Subset of High-Risk Pediatric Neuroblastomas and Is Activated through Mechanisms Including Enhancer Hijacking and Focal Enhancer Amplification.* Cancer Discov, 2018. **8**(3): p. 320-335.
5. Kulathunga, N., et al., *Peripubertal high-fat diet promotes c-Myc stabilization in mammary gland epithelium.* Cancer Sci, 2020. **111**(7): p. 2336-2348.
6. Labbe, D.P., et al., *High-fat diet fuels prostate cancer progression by rewiring the metabolome and amplifying the MYC program.* Nat Commun, 2019. **10**(1): p. 4358.
7. Gouw, A.M., et al., *The MYC Oncogene Cooperates with Sterol-Regulated Element-Binding Protein to Regulate Lipogenesis Essential for Neoplastic Growth.* Cell Metab, 2019. **30**(3): p. 556-572 e5.
8. Tao, L., et al., *MYCN-driven fatty acid uptake is a metabolic vulnerability in neuroblastoma.* Nat Commun, 2022. **13**(1): p. 3728.
9. Zirath, H., et al., *MYC inhibition induces metabolic changes leading to accumulation of lipid droplets in tumor cells.* Proc Natl Acad Sci U S A, 2013. **110**(25): p. 10258-63.
10. Rugolo, F., et al., *The expression of ELOVL4, repressed by MYCN, defines neuroblastoma patients with good outcome.* Oncogene, 2021. **40**(38): p. 5741-5751.
11. Ruiz-Perez, M.V., et al., *Inhibition of fatty acid synthesis induces differentiation and reduces tumor burden in childhood neuroblastoma.* iScience, 2021. **24**(2): p. 102128.
12. Dyall, S.C., et al., *Polyunsaturated fatty acids and fatty acid-derived lipid mediators: Recent advances in the understanding of their biosynthesis, structures, and functions.* Prog Lipid Res, 2022. **86**: p. 101165.
13. Newton, A.C., M.D. Bootman, and J.D. Scott, *Second Messengers.* Cold Spring Harb Perspect Biol, 2016. **8**(8).
14. Nagarajan, S.R., L.M. Butler, and A.J. Hoy, *The diversity and breadth of cancer cell fatty acid metabolism.* Cancer Metab, 2021. **9**(1): p. 2.
15. Horrobin, D.F., *The reversibility of cancer: the relevance of cyclic AMP, calcium, essential fatty acids and prostaglandin E1.* Med Hypotheses, 1980. **6**(5): p. 469-86.
16. Zaidi, N., et al., *Lipogenesis and lipolysis: the pathways exploited by the cancer cells to acquire fatty acids.* Prog Lipid Res, 2013. **52**(4): p. 585-9.
17. Rohrig, F. and A. Schulze, *The multifaceted roles of fatty acid synthesis in cancer.* Nat Rev Cancer, 2016. **16**(11): p. 732-749.
18. Chen, M. and J. Huang, *The expanded role of fatty acid metabolism in cancer: new aspects and targets.* Precis Clin Med, 2019. **2**(3): p. 183-191.
19. Chang, N.W., et al., *High levels of arachidonic acid and peroxisome proliferator-activated receptor-alpha in breast cancer tissues are associated with promoting cancer cell proliferation.* J Nutr Biochem, 2013. **24**(1): p. 274-81.
20. Nakazawa, I., J.F. Mead, and R.H. Yonemoto, *In vitro activity of the fatty acyl desaturases of human cancerous and noncancerous tissues.* Lipids, 1976. **11**(1): p. 79-82.
21. Okazaki, N. and E. Araki, *Eicosatrienoic acid omega9 in serum lipids of patients with hepatocellular carcinoma.* Clin Chim Acta, 1974. **53**(1): p. 11-21.

22. Park, H.G., et al., *A rare eicosanoid precursor analogue, sciadonic acid (5Z,11Z,14Z-20:3), detected in vivo in hormone positive breast cancer tissue.* Prostaglandins Leukot Essent Fatty Acids, 2018. **134**: p. 1-6.
23. Brenna, J.T. and K.S.D. Kothapalli, *New understandings of the pathway of long-chain polyunsaturated fatty acid biosynthesis.* Curr Opin Clin Nutr Metab Care, 2022. **25**(2): p. 60-66.
24. Holman, R.T. and H. Mohrhauer, *A Hypothesis Involving Competitive Inhibitions in the Metabolism of Polyunsaturated Fatty Acids.* Acta Chemica Scandivanica, 1963. **17**: p. S84-S90.
25. Johnsen, J.I., C. Dyberg, and M. Wickstrom, *Neuroblastoma-A Neural Crest Derived Embryonal Malignancy.* Front Mol Neurosci, 2019. **12**: p. 9.
26. Wang, D. and R.N. Dubois, *Eicosanoids and cancer.* Nat Rev Cancer, 2010. **10**(3): p. 181-93.
27. Kang, K.S., et al., *Docosahexaenoic acid induces apoptosis in MCF-7 cells in vitro and in vivo via reactive oxygen species formation and caspase 8 activation.* PLoS One, 2010. **5**(4): p. e10296.
28. D'Eliseo, D., et al., *Docosahexaenoic acid (DHA) promotes immunogenic apoptosis in human multiple myeloma cells, induces autophagy and inhibits STAT3 in both tumor and dendritic cells.* Genes Cancer, 2017. **8**(1-2): p. 426-437.
29. Song, E.A. and H. Kim, *Docosahexaenoic Acid Induces Oxidative DNA Damage and Apoptosis, and Enhances the Chemosensitivity of Cancer Cells.* Int J Mol Sci, 2016. **17**(8).
30. Zeller, K.I., et al., *An integrated database of genes responsive to the Myc oncogenic transcription factor: identification of direct genomic targets.* Genome Biol, 2003. **4**(10): p. R69.
31. Holman, R.T., *The ratio of trienoic: tetraenoic acids in tissue lipids as a measure of essential fatty acid requirement.* J Nutr, 1960. **70**(3): p. 405-10.
32. Zhu, Y., et al., *Antioxidant inhibition of steady-state reactive oxygen species and cell growth in neuroblastoma.* Surgery, 2015. **158**(3): p. 827-36.
33. Wang, Z., et al., *The elongation of very long-chain fatty acid 6 gene product catalyses elongation of n-13 : 0 and n-15 : 0 odd-chain SFA in human cells.* Br J Nutr, 2019. **121**(3): p. 241-248.
34. Floros, K.V., et al., *MYCN-Amplified Neuroblastoma Is Addicted to Iron and Vulnerable to Inhibition of the System Xc-/Glutathione Axis.* Cancer Res, 2021. **81**(7): p. 1896-1908.
35. Powers, J.T., et al., *Multiple mechanisms disrupt the let-7 microRNA family in neuroblastoma.* Nature, 2016. **535**(7611): p. 246-51.
36. Vienberg, S., et al., *MicroRNAs in metabolism.* Acta Physiol (Oxf), 2017. **219**(2): p. 346-361.
37. Davalos, A., et al., *miR-33a/b contribute to the regulation of fatty acid metabolism and insulin signaling.* Proc Natl Acad Sci U S A, 2011. **108**(22): p. 9232-7.
38. Nakamura, M.T. and T.Y. Nara, *Structure, function, and dietary regulation of delta6, delta5, and delta9 desaturases.* Annu Rev Nutr, 2004. **24**: p. 345-76.
39. Safa, A., et al., *miR-1: A comprehensive review of its role in normal development and diverse disorders.* Biomed Pharmacother, 2020. **132**: p. 110903.
40. Zhao, N., et al., *MicroRNA-1 affects the development of the neural crest and craniofacial skeleton via the mitochondrial apoptosis pathway.* Exp Ther Med, 2021. **21**(4): p. 379.
41. Wang, J., et al., *Molecular mechanisms and clinical applications of miR-22 in regulating malignant progression in human cancer (Review).* Int J Oncol, 2017. **50**(2): p. 345-355.
42. Guo, J., et al., *Identification of miRNAs that are associated with tumor metastasis in neuroblastoma.* Cancer Biol Ther, 2010. **9**(6): p. 446-52.

43. Buechner, J., et al., *Tumour-suppressor microRNAs let-7 and mir-101 target the proto-oncogene MYCN and inhibit cell proliferation in MYCN-amplified neuroblastoma.* Br J Cancer, 2011. **105**(2): p. 296-303.
44. Beckers, A., et al., *MYCN-driven regulatory mechanisms controlling LIN28B in neuroblastoma.* Cancer Lett, 2015. **366**(1): p. 123-32.
45. Welch, C., Y. Chen, and R.L. Stallings, *MicroRNA-34a functions as a potential tumor suppressor by inducing apoptosis in neuroblastoma cells.* Oncogene, 2007. **26**(34): p. 5017-22.
46. Feng, J., et al., *miR-150 functions as a tumour suppressor in human colorectal cancer by targeting c-Myb.* J Cell Mol Med, 2014. **18**(10): p. 2125-34.
47. Kosti, A., et al., *ELF4 Is a Target of miR-124 and Promotes Neuroblastoma Proliferation and Undifferentiated State.* Mol Cancer Res, 2020. **18**(1): p. 68-78.
48. Mizuno, K., et al., *Regulation of Oncogenic Targets by Tumor-Suppressive miR-150-3p in Lung Squamous Cell Carcinoma.* Biomedicines, 2021. **9**(12).
49. Ryan, J., et al., *MicroRNA-204 increases sensitivity of neuroblastoma cells to cisplatin and is associated with a favourable clinical outcome.* Br J Cancer, 2012. **107**(6): p. 967-76.
50. Agbaga, M.P., et al., *Role of Stargardt-3 macular dystrophy protein (ELOVL4) in the biosynthesis of very long chain fatty acids.* Proc Natl Acad Sci U S A, 2008. **105**(35): p. 12843-8.
51. Stallings, R.L., *MicroRNA involvement in the pathogenesis of neuroblastoma: potential for microRNA mediated therapeutics.* Curr Pharm Des, 2009. **15**(4): p. 456-62.
52. Fang, R., et al., *MicroRNA-143 (miR-143) regulates cancer glycolysis via targeting hexokinase 2 gene.* J Biol Chem, 2012. **287**(27): p. 23227-35.
53. Singh, P.K., et al., *Regulation of Aerobic Glycolysis by microRNAs in Cancer.* Mol Cell Pharmacol, 2011. **3**(3): p. 125-134.
54. Smith, R.L., et al., *Metabolic Flexibility as an Adaptation to Energy Resources and Requirements in Health and Disease.* Endocr Rev, 2018. **39**(4): p. 489-517.
55. Aravindan, N., et al., *MicroRNAs in neuroblastoma tumorigenesis, therapy resistance, and disease evolution.* Cancer Drug Resist, 2019. **2**(4): p. 1086-1105.
56. Mei, H., Z.Y. Lin, and Q.S. Tong, *The roles of microRNAs in neuroblastoma.* World J Pediatr, 2014. **10**(1): p. 10-6.
57. Jin, H.Y. and C. Xiao, *MicroRNA Mechanisms of Action: What have We Learned from Mice?* Front Genet, 2015. **6**: p. 328.
58. Baskerville, S. and D.P. Bartel, *Microarray profiling of microRNAs reveals frequent coexpression with neighboring miRNAs and host genes.* RNA, 2005. **11**(3): p. 241-7.
59. Zhang, L., C. Li, and X. Su, *Emerging impact of the long noncoding RNA MIR22HG on proliferation and apoptosis in multiple human cancers.* J Exp Clin Cancer Res, 2020. **39**(1): p. 271.
60. Nishida, K., Y. Kuwano, and K. Rokutan, *The MicroRNA-23b/27b/24 Cluster Facilitates Colon Cancer Cell Migration by Targeting FOXP2.* Cancers (Basel), 2020. **12**(1).
61. Teitelbaum, D.H., et al., *Proceedings From FDA/A.S.P.E.N. Public Workshop: Clinical Trial Design for Intravenous Fat Emulsion Products, October 29, 2013.* JPEN J Parenter Enteral Nutr, 2015. **39**(7): p. 768-86.
62. Cunnane, S.C. and M.J. Anderson, *Pure linoleate deficiency in the rat: influence on growth, accumulation of n-6 polyunsaturates, and [1-14C]linoleate oxidation.* J Lipid Res, 1997. **38**(4): p. 805-12.
63. Wang, Y., et al., *ALOX5 exhibits anti-tumor and drug-sensitizing effects in MLL-rearranged leukemia.* Sci Rep, 2017. **7**(1): p. 1853.

64. Heyd, V.L. and A.R. Eynard, *Effects of eicosatrienoic acid (20:3 n-9, Mead's acid) on some promalignant-related properties of three human cancer cell lines.* Prostaglandins Other Lipid Mediat, 2003. **71**(3-4): p. 177-88.
65. Eynard, A.R., W.G. Jiang, and R.E. Mansel, *Eicosatrienoic acid (20:3 n-9) inhibits the expression of E-cadherin and desmoglein in human squamous cell carcinoma in vitro.* Prostaglandins Leukot Essent Fatty Acids, 1998. **59**(6): p. 371-7.
66. Kothapalli, K., H.G. Park, and J.T. Brenna, *FADS2 Function at the Major Cancer Hotspot 11q13 Locus Alters Fatty Acid Metabolism in Cancer.* Preprints.org, 2022: p. 2022100206.
67. Park, W.J., et al., *An alternate pathway to long-chain polyunsaturates: the FADS2 gene product Delta8-desaturates 20:2n-6 and 20:3n-3.* J Lipid Res, 2009. **50**(6): p. 1195-202.
68. Gregory, M.K., et al., *Elongase reactions as control points in long-chain polyunsaturated fatty acid synthesis.* PLoS One, 2011. **6**(12): p. e29662.
69. Park, H.G., et al., *Palmitic acid (16:0) competes with omega-6 linoleic and omega-3 a-linolenic acids for FADS2 mediated Delta6-desaturation.* Biochim Biophys Acta, 2016. **1861**(2): p. 91-97.
70. West, L., et al., *Docosahexaenoic acid (DHA), an omega-3 fatty acid, inhibits tumor growth and metastatic potential of ovarian cancer.* Am J Cancer Res, 2020. **10**(12): p. 4450-4463.
71. Yin, Y., et al., *The omega-3 polyunsaturated fatty acid docosahexaenoic acid inhibits proliferation and progression of non-small cell lung cancer cells through the reactive oxygen species-mediated inactivation of the PI3K /Akt pathway.* Lipids Health Dis, 2017. **16**(1): p. 87.
72. Zhao, H., et al., *Inflammation and tumor progression: signaling pathways and targeted intervention.* Signal Transduct Target Ther, 2021. **6**(1): p. 263.
73. Xiao, L., et al., *Immunometabolism: A 'Hot' Switch for 'Cold' Pediatric Solid Tumors.* Trends Cancer, 2021. **7**(8): p. 751-777.
74. Wolpaw, A.J., et al., *Epigenetic state determines inflammatory sensing in neuroblastoma.* Proc Natl Acad Sci U S A, 2022. **119**(6).
75. Bae, S., et al., *Arachidonic acid induces ER stress and apoptosis in HT-29 human colon cancer cells.* Anim Cells Syst (Seoul), 2020. **24**(5): p. 260-266.
76. Li, W., et al., *The prognostic value of arachidonic acid metabolism in breast cancer by integrated bioinformatics.* Lipids Health Dis, 2022. **21**(1): p. 103.
77. Doll, S., et al., *ACSL4 dictates ferroptosis sensitivity by shaping cellular lipid composition.* Nat Chem Biol, 2017. **13**(1): p. 91-98.
78. Liao, P., et al., *CD8(+) T cells and fatty acids orchestrate tumor ferroptosis and immunity via ACSL4.* Cancer Cell, 2022. **40**(4): p. 365-378 e6.
79. Viswanathan, S.R., G.Q. Daley, and R.I. Gregory, *Selective blockade of microRNA processing by Lin28.* Science, 2008. **320**(5872): p. 97-100.
80. Wang, Z., et al., *Fatty acid desaturase 2 (FADS2) but not FADS1 desaturates branched chain and odd chain saturated fatty acids.* Biochim Biophys Acta Mol Cell Biol Lipids, 2020. **1865**(3): p. 158572.
81. Park, H.G., et al., *The role of fatty acid desaturase (FADS) genes in oleic acid metabolism: FADS1 Delta7 desaturates 11-20:1 to 7,11-20:2.* Prostaglandins Leukot Essent Fatty Acids, 2018. **128**: p. 21-25.
82. Park, H.G., et al., *The fatty acid desaturase 2 (FADS2) gene product catalyzes Delta4 desaturation to yield n-3 docosahexaenoic acid and n-6 docosapentaenoic acid in human cells.* FASEB J, 2015. **29**(9): p. 3911-9.
83. Garces, R. and M. Mancha, *One-step lipid extraction and fatty acid methyl esters preparation from fresh plant tissues.* Anal Biochem, 1993. **211**(1): p. 139-43.

84. Wang, D.H., et al., *Characterization and Semiquantitative Analysis of Novel Ultratrace C10-24 Monounsaturated Fatty Acid in Bovine Milkfat by Solvent-Mediated Covalent Adduct Chemical Ionization (CACI) MS/MS.* J Agric Food Chem, 2020. **68**(28): p. 7482-7489.
85. Van Pelt, C.K. and J.T. Brenna, *Acetonitrile chemical ionization tandem mass spectrometry to locate double bonds in polyunsaturated fatty acid methyl esters.* Anal Chem, 1999. **71**(10): p. 1981-9.